# Mechanical studies of irradiation-induced defects in Cu and W†

J. R. Townsend, M. Schildcrout,* and C. Reft‡
*Department of Physics, University of Pittsburgh, Pittsburgh, Pennsylvania 15260*
(Received 27 May 1975)

Measurements of internal friction and Young's elastic modulus in the kilohertz range are reported on single-crystal and polycrystalline Cu and W samples after irradiation by 10- to 14-MeV protons and deuterons, primarily at temperatures near 4 K. Stress-induced ordering studies in Cu identify stage $I_B$ as responsible for the 10-K anelastic process; a shape factor $\Delta\lambda = 0.20 \pm 0.02$ was found for this defect. W shows anelastic peaks near 10, 14, 30, 42, and 53 K. The 10- and 30-K peaks are removed by a 40-K anneal, the 14-K peak is created by this same anneal. Attempt frequencies and activation energies for reorientation are reported for these defects. Dielastic effects seem unaffected by cold work, but the 10-K peaks are totally suppressed in both Cu and W by a plastic compression of 10 to 20%. Dielastic effects anneal out in stage I in Cu, while only about 1/3 of the effect anneals out in W by an anneal to 50 K. Cold work has a large effect upon the amount and rate of pinning, especially in Cu. Cold work also seems to reduce the role of thermally activated defect motion in the pinning process.

## I. INTRODUCTION

Reported here are results of measurements on the mechanical properties of Cu and W samples before and after irradiation at low temperatures, by 10- to 15-MeV protons or deuterons. Measurements of internal friction and Young's elastic modulus have resulted in quantitative and qualitative information on stress-induced ordering, dislocation pinning, and elastic-modulus change by bulk and polarization effects produced by irradiation of these two metals. All of these effects in metals have been attributed to the production of interstitials and vacancies, so they become useful tools for the study of these defects.

Stress-induced ordering refers to the anelastic process which may result from the interaction energy between an applied stress and the internal strain field of a defect.[1] If certain atomic arrangements are energetically favored in the presence of an applied stress, then a classic Debye type of relaxation process is observed when the atomic arrangement relaxation time $\tau_r$ is close to the period of an alternating applied stress. Because the relaxation is typically achieved by a thermally activated atomic jump process

$$\tau_r^{-1} = \nu_0 \exp(-Q_r/kT) , \tag{1}$$

where $Q_r$ is the activation energy for the atomic rearrangement and $\nu_0$ is the reorientation frequency with zero activation energy. When the sample is subjected to an alternating stress of angular frequency $\omega$, then for a single $\tau_r$ a Debye relaxation process gives

$$\delta = \pi\Delta_0\omega\tau_r/[1+(\omega\tau_r)^2] , \tag{2}$$

$$\Delta M/M = -\Delta_0/[1+(\omega\tau_r)^2] , \tag{3}$$

where $\delta$ is the logarithmic decrement, $\Delta M$ is the change in the elastic modulus relative to the unrelaxed (low-temperature) value, and $\Delta_0$ is the relaxation strength. Combining Eqs. (1) and (2), one can show that for a peak with its maximum at $T_m$,

$$\Delta T_0 = (k/Q_r)T_m^2 2.63 \tag{4}$$

is the temperature width of the peak at its half-maximum. This serves as a test of the applicability of a single Debye relaxation process. As discussed at length by Nowick and Berry,[1] and using the notation of DiCarlo *et al.*[2] to make it easier to compare their results with ours

$$\Delta_0 = (Cv_0 M^{[hkl]}/9kT)\psi^{[hkl]}_{(uvw)} , \tag{5}$$

where $C$ is the atomic fraction of participating defects, $v_0$ is the atomic volume, $[hkl]$ denotes the crystal direction of the applied uniaxial stress, and $(uvw)$ is the crystallographic orientation of the defect's principal axis of elastic distortion. In the present case of Cu and W, the defect axes of interest lie along the $\langle 111\rangle$ and the $\langle 110\rangle$ directions, respectively. As summarized by DiCarlo *et al.*, $\psi$ can be expressed in terms of the defect strain tensor components $\lambda_1$, $\lambda_2$, $\lambda_3$. The essential results for the present work are summarized in Table I.

Dislocation pinning is made evident by the removal of their anelastic effects.[3] Their motion under an applied stress produces both a background type of anelastic process which increases monotonically with temperature and a Debye type of relaxation process which produces a "Bordoni peak" in $\delta$. By interacting with the dislocation strain field, irradiation induced defects increasingly hinder dislocation motion thereby diminishing their anelastic contributions. While extensive theoretical and experimental work has been done on this dramatic effect,[3-5] especially in the case of Cu, interpretations of the results continue to be primari-

TABLE I. Defect strain tensors.

| Defect axis | Principal stain directions | $\psi^{a}$ |
|---|---|---|
| ⟨111⟩ (as found in Cu 10-K peak) | $\lambda_1$, $\lambda_2 = \lambda_3$ ⟨111⟩ ⟨1$\bar{1}$0⟩ ⟨11$\bar{2}$⟩ | $\psi_{111}^{100}=0$ <br> $\psi_{111}^{111}=\frac{4}{3}(\lambda_1-\lambda_2)^2$ |
| ⟨110⟩ (as assumed for W 10- and 30-K peaks) | $\lambda_1$, $\lambda_2$, $\lambda_3$ ⟨110⟩, ⟨1$\bar{1}$0⟩, ⟨001⟩ | $\psi_{110}^{100}=\frac{1}{2}(\lambda_1-\lambda_3+\lambda_2-\lambda_3)^2$ <br> $\psi_{110}^{111}=(\lambda_1-\lambda_2)^2$ |

[a] $\psi_{uvw}^{110}$ can be found by the theoretical relationship $\psi_{uvw}^{110}=\frac{1}{4}\psi_{uvw}^{100}+\frac{3}{4}\psi_{uvw}^{111}$.

ly semiquantitative.

The linear decrease in the elastic moduli as irradiation continues has been associated with the accumulation of defects throughout the volume of a crystal. These defects, without undergoing lattice jumps, change the local lattice response to an applied stress. These effects upon the elastic modulus have been referred to as the bulk effect; more recently Wenzl[6] has reviewed these changes under the name of "dielastic effect." Recent experimental[7] and theoretical[8] results on this effect for Cu strongly suggest that easily deformed split interstitials are primarily responsible.

## II. EXPERIMENTAL PROCEDURES

While many changes in detail were made, the procedure was essentially that described earlier.[9] A major change in the sample cryostat permitted liquid-helium temperatures to be reached. Figure 1 shows schematically the bottom of the cryostat and the sample mounting on the PZT bimorph, a piezoelectric transducer supplied by Clevite Corporation. An unfortunate feature of the design was the close proximity of the heater and the leads for the Pt resistance thermometer. When a helium heat exchange gas was present during some anneal runs, excess heat flowed down the lead wire to the Pt thermometer thereby giving a "temperature" reading that was too high. This temperature excess ranged from zero at 4.2 K to 2 °K at an apparent temperature of 11 K and approximately 3 °K at apparent temperatures above 15 K. This systematic error was absent when no gas was used. A second sample probe was built incorporating a carbon resistance thermometer as well as a new location for the heater; results with this probe verified the temperature corrections which have been applied, especially below 15 K. In general the temperature errors on a given run tended to be constant above 12 K; thus temperature differences on a given run were reliable to ±0.2 K. The absolute temperatures with no gas present are accurate to ±0.5 K. The temperatures measured with a gas can be corrected to ±0.5 K up to 15 K and to ±1 K above 15 K.

The bimorph signal was filtered through a low-$Q$ electrical filter, amplified and phase shifted as needed before being fed back to drive the sample in a steady state at one of its resonant frequencies. The sample was driven either electrostatically (by a drive plate near the free end) or magnetically (by an electromagnet exerting a force on a small piece of soft iron wire cemented to the free end of the sample). The resonance frequency $f$ was measured on a Hewlett Packard frequency counter, the log decrement $\delta$ was normally measured to ±5% during free decay by a procedure described by Swartz.[10] Because the resonant frequency is proportional to $E^{1/2}$,

$$\Delta f/f_0 \cong \Delta E/2E_0 , \tag{6}$$

where $E$ is Young's elastic modulus. Values of $\Delta f/f$ were reproducible to $\pm 1\times10^{-5}$. Maximum strain amplitudes ranged from $5\times10^{-7}$ to $5\times10^{-6}$. While small amounts of amplitude dependence were occasionally seen in $f$ and $\delta$ for the well annealed samples, the importance of this effect was mini-

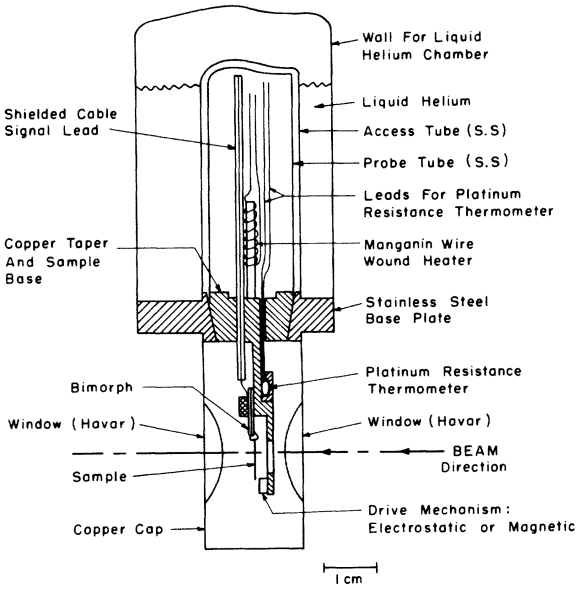


FIG. 1. Schematic drawing of sample mounting.

TABLE II. Sample information

| Sample | No.[a] | Type (see text) | $f_0$(Hz)[b] | Remarks[a] |
|---|---|---|---|---|
| Cu | 1 | *A* | 850, 5220(OT) | Px; 650°C, CW-2; 2.5, 9-MeV p; 1.39 |
| | 2 | | 1050 | Px; 650°C, CW-2; 1.25 anneal to 80 K, 2nd irrad 2.25, both 9-MeV p; 1.39 |
| | 155 | | 950 | Px; 650°C, CW-2; 7.0, 9 meV *p*; 1.39 |
| | 200 | *B* | 1600 | ⟨100⟩; *nc* anneal, CW-2; 5.5, 9-MeV *p*; 1.63 |
| | 203 | | 2060 | ⟨111⟩; no anneal, CW-2; 3.3, 9-MeV *p*; 1.69 |
| | 3 | *C* | 704 | ⟨100⟩; 800°C, CW-2; 1.0 at 73 K; 1.26 |
| | 4 | | 920 | ⟨110⟩; no anneal, CW-25%; 3.0; 1.23 |
| | 5 | | 1107 | ⟨110⟩; no anneal, CW-25%; 3.0; 1.23 |
| | 6 | | 1070 | ⟨110⟩; 480°C, CW-2; 1.75; 1.20 |
| | 7 | | 1970 | ⟨110⟩; 480°C, CW-2; 3.0; 1.30 |
| | 8 | | 730 | ⟨111⟩; 480°C, CW-2, 1.5; 1.20 |
| | 9 | | 852 | ⟨111⟩; 750°C, CW-3; 1.6; 1.17 |
| | 10 | | 1270, 5960(OT) | ⟨111⟩; 800°C, CW-1; 1.35; 1.24 |
| W | 300 | *G* | 1560 | Px; 1600°C, CW-2; 4.0, 9-MeV *p*; 1.48 |
| | 301 | | 790 | Px; 1550°C, CW-2; 3.0, 9-MeV *p*; 1.48 |
| | 302[c] | | 775, 4840(OT) | Px; 1550°C, CW-2; 1.0, annealed to 50 K, 2nd irrad. 2.6, both 11.1-MeV *p*; 0.93 |
| | 351[d] | | 745, 4850(OT) | Px; 1500°C, CW-2; 6.5, annealed to 53 K 2nd irrad. 3.0; 11.1-MeV *p*; 1.0 |
| | 11[d] | | 2250(OT) | Px; 2000°C, CW-2; 3.7, 11.1 MeV *p*; 1.0 |
| | 12 | *H* | 830 | ⟨110⟩; 1 h at 1200°C, CW-1, 0.46, 14-MeV *d*; 1.38 |
| | 13 | | 720 | ⟨110⟩; 1460°C; CW-1; 1.4; 1.2 |
| | 14 | | 858 | ⟨110⟩; no anneal, CW-2; 2.50; 1.2 |
| | 15 | | 720, 5140(OT) | ⟨110⟩; no anneal, 3%; 1.4; 1.2 |
| | 16 | | 3585(OT) | ⟨110⟩; no anneal, 4%; 3.6; 1.2 |
| | 17 | | 1030 | ⟨110⟩; no anneal, 4%; 0.5; 14-MeV *d*; 1.8 |
| | 18 | | 800 | ⟨110⟩; no anneal, 5%; 2.5; 1.2 |
| | 19 | | 990, 5300(OT) | ⟨110⟩; no anneal, 5%; 2.0; 1.2 |
| | 20 | | 830, 5180(OT) | ⟨110⟩; no anneal, 13%; 2.0; 1.1 |
| | 500 | | 1730 | ⟨110⟩; no anneal, CW-2; 3.6, 11.1-MeV *p*; 1.10 |
| | 600 | | 1700 | ⟨111⟩; no anneal, CW-2; 3.6, 11.1-MeV *p*; 1.10 |
| | 700 | | 1380, 9090(OT) | ⟨110⟩; no anneal, CW-2; 3.6, 11.1-MeV *p*; 1.05 |

[a]Sample Nos. 1–20 are new samples, other samples and all sample types have been referred to earlier in Ref. 11 and 13.

[b]Preirradiation resonant frequency, OT denotes first overtone.

[c]Etched from 0.010- to 0.003-cm diameter after anneal.

[d]Diameter reduced from 0.010 to 0.008 cm by rolling at room temperature, then annealed, then etched to 0.006 cm.

[e]In order of appearance under Remarks: orientation if single crystal or Px for polycrystal; vacuum anneal temperature and cold-work condition (qualitative categories as in text or % compression at room temperature); total fluence in units of $10^{16}$ particles $cm^2$, 10.1-MeV protons at 4.2 K unless noted otherwise (*p* denotes protons, *d* denotes deuterons); $F_y$ energy-loss correction factor (see text).

mized by using the same amplitude while studying a given sample. Amplitude dependence was never observed for the stress-induced ordering phenomena.

Sample irradiations took place in the University of Pittsburgh's tandem Van de Graaff accelerator. Beam energies were known from routine nuclear physics instrumentation; energy corrections for window foils were made using standard stopping power tables. Over all, beam energies incident on the samples were known to ±0.1 MeV. Fluences were calculated from the integrated current collected by a Faraday cup using the known area of the liquid-nitrogen collimator which was about 1 cm long and 0.3 cm wide.

During liquid-helium irradiations by particle fluxes up to 0.2 $\mu A/cm^2$, the sample temperature remained below 15 K as determined by the change in the sample's resonant frequency when the beam was interrupted. Uniformity of beam over the sample and the collimator was assured by small angle scattering from a 0.0005-in. Havar foil located about 30 cm from the sample and by defocussing the beam so the current was balanced on four

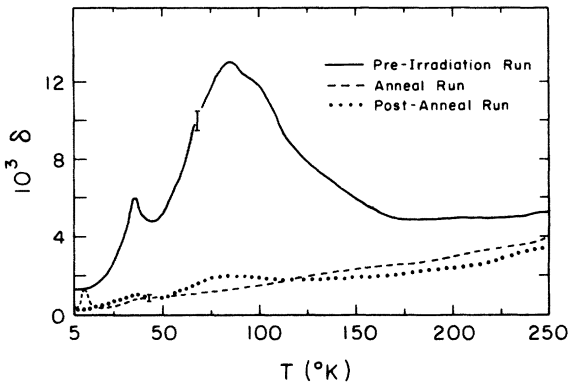


FIG. 2. Log decrement $\delta$ vs temperature for typical Cu sample. Anneal run followed irradiation by 9-MeV protons, post-anneal run followed anneal run.

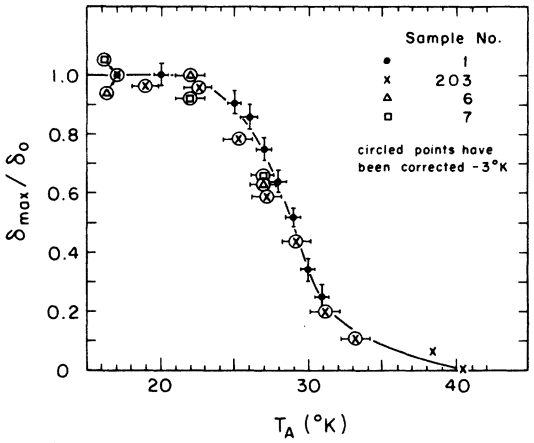


FIG. 4. Relative 10-K peak height in Cu vs anneal temperature. Anneals were for 10 min at $T_A$.

monitoring slits which surrounded the collimator.

### A. Samples

Single-crystal samples were nearly rectangular in shape; polycrystalline wire samples were either round or were slightly flattened to assure a well defined vibration mode. The dimension traversed by the charged particles ranged from 0.002 to 0.010 cm; widths from 0.025 to 0.075 cm; lengths from 0.5 to 1.5 cm. Samples were fastened to the bimorph either with the cement directly holding the stationary end of the bar or a sharp step in the thickness was made in the sample and the thicker section was then cemented to the bimorph. The latter method was preferable for it gave more stability during cycling to room temperature. Aside from this feature, both methods gave identical results.

The Cu samples were of three types: *A*, samples 1, 2, and 155 0.013-cm-diam wire, flattened to 0.010 cm thick by rolling, vacuum annealed to

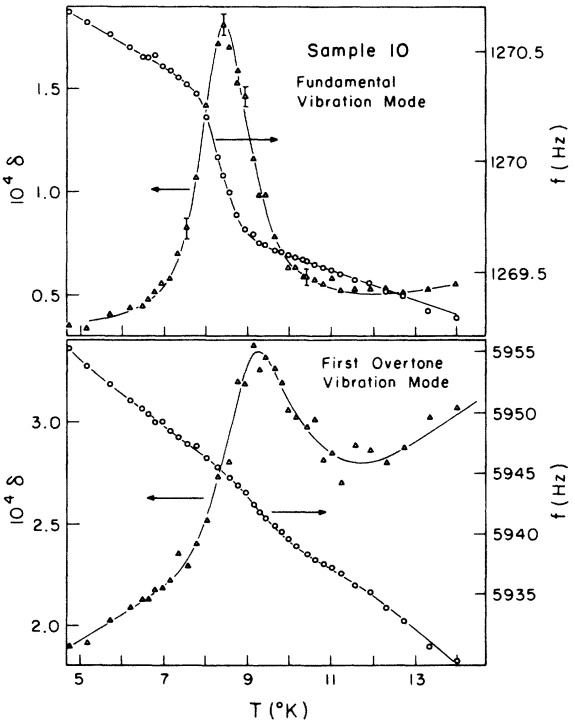


FIG. 3. $\delta$ and $f$ vs temperature for a Cu single-crystal sample following irradiation near liquid-helium temperature. Top figure shows fundamental vibration mode; bottom figure shows first overtone results.

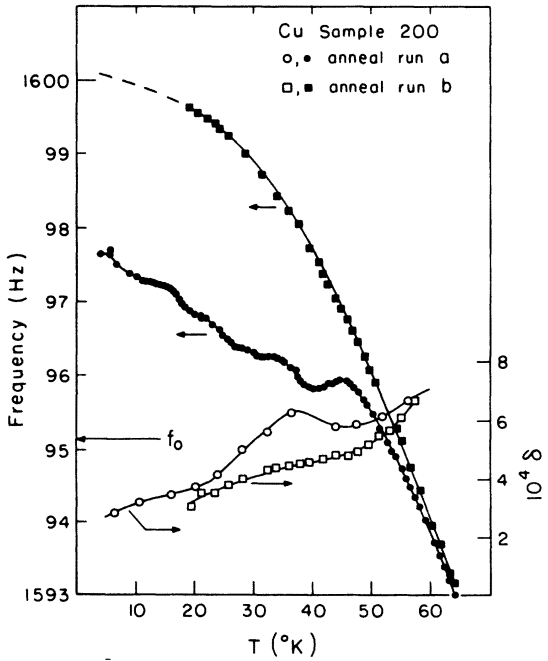


FIG. 5. Two successive anneal runs following irradiation of a ⟨100⟩ Cu single crystal. Anneal run *a* up to 59 K immediately followed by anneal run *b*. Absence of 10-K peak in $\delta$ is noteworthy.

TABLE III. Peak data.

| | Sample[a] | $T_M$[b] | Normalized $10^4\delta_0$[a] | $\Delta T$(K)[d] | $\Delta T_0$(°K)[e] | |
|---|---|---|---|---|---|---|
| Cu | 10(F) | 8.40 | 8.2 ± 0.2 | 1.40 ± 0.02 | 1.14 | $\Delta f/f_0^c = (2.75 \pm 0.05) \times 10^{-4}$ |
| | 10(OT) | 9.22 | 5.6 ± 0.2 | 1.8 ± 0.3 | 1.37 | |
| | 1(F) | 9.4 | 1.9 ± 0.2 | 2.7 ± 0.2 | | $\Delta f/f_0^c = (0.97 \pm 0.05) \times 10^{-4}$ |
| | 1(OT) | 10.4 | 1.0 ± 0.3 | 1.9 ± 0.4 | | |
| | 9 | 9.0 | 1.2 ± 0.1 | 1.9 ± 0.2 | | |
| | 6 | 8.9 | 2.0 ± 0.1 | 2.1 ± 0.1 | | |
| | 5 | | < 0.2 | | | 25% compression |
| | 200 | | < 0.04 | | | ⟨100⟩ orientation |
| W | 12 | 10 ± 1 | 1.9 ± 0.4 | 2.0 ± 0.3 | | $\Delta f/f_0^c = (1.05 \pm 0.03) \times 10^{-4}$ |
| | 302 | 10.5 | 1.5 ± 0.1 | 2.3 ± 0.2 | 1.25 | $\Delta f/f_0^c = (0.74 \pm 0.02) \times 10^{-4}$ |
| | 302(OT) | 11.8 | 1.3 ± 0.1 | 2.2 ± 0.2 | 1.50 | |
| | 351(F) | 10.3 | 0.55 ± 0.05 | 3.8 ± 0.2 | | first irradiation |
| | 351(OT) | 11.5 | 0.45 ± 0.05 | 3.5 ± 0.2 | | first irradiation |
| | 351(F) | | 0.61 ± 0.05 | 3.8 ± 0.2 | | second irradiation |
| | 351(OT) | 10.3 | 0.53 ± 0.05 | 4.2 ± 0.2 | | second irradiation |
| | 700(F) | 10.3 | 0.52 ± 0.03 | 2.9 ± 0.2 | | $\Delta f/f_0^c = (0.2 \pm 0.05) \times 10^{-4}$ |
| | 700(OT) | 11.5 | | 3.8 ± 0.2 | | |
| | 600 | 10.5 | 0.46 ± 0.03 | 2.6 ± 0.2 | | $\Delta f/f_0^c = (0.30 \pm 0.05) \times 10^{-4}$ |
| | 500 | 10.0 | 1.10 ± 0.05 | 2.7 ± 0.2 | | $\Delta f/f_0^c = (0.86 \pm 0.06) \times 10^{-4}$ |
| | 20 | | < 0.05 | | no peak seen, $\Delta f/f_0^c < 0.25 \times 10^{-4}$ | |
| | 302(F) | 13.9 ± 0.1 | 0.19 ± 0.01 | 1.8 ± 0.2 | 2.06 | |
| | 302(OT) | 15.5 ± 0.1 | 0.20 ± 0.01 | 2.6 ± 0.2 | 2.56 | |
| | 302(F) | 30.0 | 2.1 ± 0.3 | 5.5 ± 0.3 | 3.34 | annealing during observation |
| | 302(OT) | 32.5 | 1.1 ± 0.2 | 5.5 ± 0.3 | 3.82 | |
| | 351(F) | 28.5 | | | | first irradiation |
| | 351(OT) | 31.0 | | | | first irradiation |
| | 351(F) | 29.4 | | | | second irradiation |
| | 351(OT) | 32.3 | | | | second irradiation |
| | 700 | 29.0 | 2.07 ± 0.05 | | | |
| | 600 | 29.8 | 1.07 ± 0.02 | | | |
| | 500 | | 7.6 ± 0.1 | 6.5 ± 0.4 | | first warm up to 30 K |
| | 500 | 30.5 | 5.7 ± 0.1 | 7.5 ± 0.2 | | second warm up |
| | 302(F) | 53.5 ± 0.4 | 0.47 ± 0.04 | 8.3 ± 0.8 | 4.90 | $\delta_0$ normalized assuming 50 K |
| | 302(OT) | 57.0 ± 0.4 | | | 5.70 | anneal did not affect $\delta_0$ |
| | 351(F) | 53.2 ± 0.4 | 0.19 ± 0.02 | 6.8 ± 0.8 | | $\delta_0$ normalized assuming |
| | 351(OT) | 57.3 ± 0.4 | 0.14 ± 0.02 | 6.3 ± 0.8 | | 53 K anneal did not affect $\delta_0$ |
| | 700 | 55 ± 1 | 0.17 ± 0.02 | | | |
| | 600 | 55 ± 1 | 0.23 ± 0.02 | | | |
| | 500 | 55.8 ± 0.4 | 0.74 ± 0.03 | | | |

[a] F and OT denote fundamental and first overtone modes for same warm up.
[b] Uncertainty in $T_M$ is ±0.2 K unless otherwise noted.
[c] Normalized to $10^{16}$ protons/cm$^2$ at 10 MeV for zero sample thickness.
[d] Observed temperature width of peak at half-maximum.
[e] Based on Eq. (4) using $Q_r$ from Table IV.

above 600 °C, supplied by Sigmund Cohn Corp., 99.999% pure; *B*, these samples were spark cut from a large bar to 0.075 cm square bars, then etched to 0.013 cm on a side, no anneal; *C*, these were spark cut from a Marz grade (99.999%) cylinder from Materials Research Corporation, they were then etched, electropolished and annealed to various temperatures at a pressure of $< 10^{-6}$ Torr and finally subjected to various degrees of cold work as noted in Table II.

The W samples were of two types: (*G*) Allied Chemical 0.013 cm. diameter wire, less than 10 ppm of the common impurities and about 50 ppm of fluorine; (*H*) samples spark cut and then etched from a Marz grade cylinder from Materials Research Corporation, treated like samples of type (*C*) copper.

Crystallographic orientations for the single-crystal samples refer to the long axis of the cantilevered bar along which the essentially uniaxial stresses were acting as the sample vibrated. These orientations were within 3° as determined by x-ray

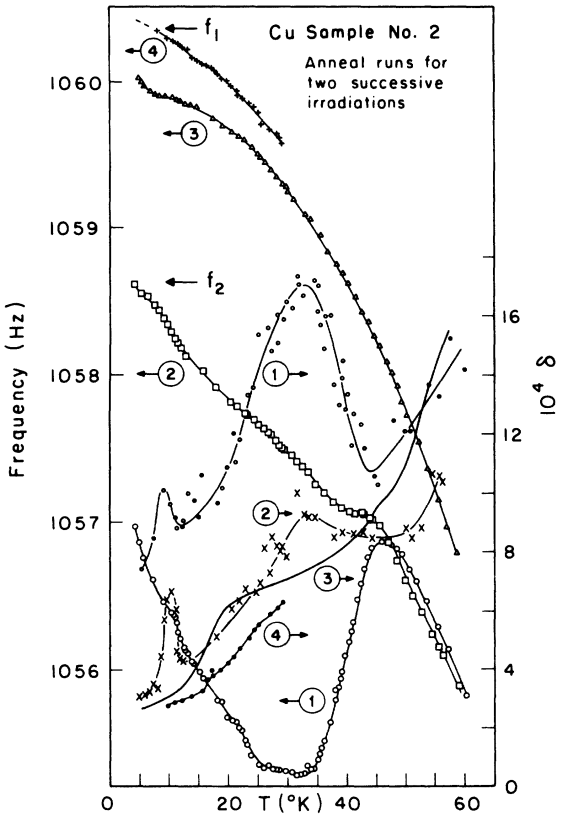


FIG. 6. $\delta$ and $f$ vs $T$ for Cu sample 2. (1) denotes warm-up following $\phi = 1.25\times10^{16}$ of 9-MeV protons at $T<15$ K. A brief anneal to 80 K resulted in frequency $f_1$ being measured at 4.2 K. A second irradiation of $\phi = 2.25\times10^{15}$ cm$^2$ at $T<15$ K lowered the frequency to $f_2$ by a dielastic effect linear in $\phi$. (2), (3), and (4) denote three successive warm-ups to 60 K. Note that the frequency at 4.2 K returned to $f_1$.

diffraction using back reflection and full rotation photographs.

The cold-work (CW) specifications in Table II are of two types. One consists of the percent reduction in thickness produced by room-temperature compression. The other specification is more qualitative consisting of CW-1, -2, or -3. For CW-1 the samples were carefully annealed and no observable CW was introduced during the mounting process. CW-2 contains samples which had received moderate CW either during the mounting or as a result of wire drawing or spark cutting damage which did not fully anneal out. This category showed Bordoni peak structures analogous to samples having plastic strains of about (2–5)%. CW-3 contains Cu samples which were heavily deformed by bending.

For most samples the energy loss of the charged particles is 40% or less, but even then the density of damage will vary from front to rear. For comparison of the results from different samples, and also with theoretical predictions, corrections must be made for this variation. The corrections as made here transform the experimental result into what would have been observed with 10-MeV protons incident upon a sample of zero thickness. For changes in $\delta$ or frequency which are linear in the fluence, the details of this correction have been discussed elsewhere.[11] The result is a factor $F_y$ (see Table II) which is very close to the energy ratio $10/E_c$ with $E_c$ being the energy of the particle at the sample's midplane. If deuterons are used, $F_y$ has another factor of 2. Where the correction is appropriate, the observed value divided by $F_y$ gives the corrected value. This type of correction

TABLE IV. Defect characteristics.

| Defect | $Q_r$(eV)[a] | $\log_{10}\nu_0$[a] | Shape factors[b] | Comments |
|---|---|---|---|---|
| Cu (10K) (stage I-b, close pair) | 0.014 ± 0.002 | 11.7 ± 1 | $\lvert\lambda_1-\lambda_2\rvert = 0.20$ | $\lambda_1 = 0.77$ |
| | | | | $\lambda_2=\lambda_3 = 0.57$ |
| W(10 K) | 0.016 ± 0.001 | 11.8 ± 0.5 | $\lambda_1-\lambda_2 = 0.034$ | observed: $R_{100}^{110} = 0.41 \pm 0.02$, $R_{100}^{111} = 0.36 \pm 0.02$[c] |
| | | | $\lambda_1-\lambda_3 = 0.062$ | refined: $R_{100}^{110} = 0.48 \pm 0.01$, $R_{100}^{111} = 0.30 \pm 0.01$[d] |
| | | | | $\lambda_1 = 0.32$, $\lambda_2 = 0.29$, $\lambda_3 = 0.26$ |
| W(14 K) | 0.021 ± 0.002 | 11.4 ± 1 | | |
| W(30 K) | 0.057 ± 0.003 | 13.5 ± 1 | $\lambda_1-\lambda_2 = 0.046$ | observed: $R_{100}^{110} = 0.27 \pm 0.01$, $R_{100}^{111} = 0.14 \pm 0.01$[c] |
| | | | $\lambda_1\ \lambda_3 = 0.117$ | refined: $R_{100}^{110} = 0.34 \pm 0.01$, $R_{100}^{111} = 0.12 \pm 0.01$[d] |
| | | | | $\lambda_1 = 0.34$, $\lambda_2 = 0.30$, $\lambda_3 = 0.22$ |
| W(53 K) | 0.130 ± 0.003 | 15.8 ± 1 | | |

[a]Based on F and OT values of $T_M$ measured on the same warm ups (see Table III) and using Eq. (9).
[b]Shape factors are accurate to an estimated 10% corresponding to a 20% uncertainty in defect concentrations.
[c]As defined by DiCarlo *et al.* $R_{100}^{hkl}$ = ratio of $\Delta_0^{hkl}/\Delta_0^{100}$.
[d]Refined by requiring $4R_{100}^{110} - 3R_{100}^{111} = 1$, assumes an orthorhombic defect symmetry.

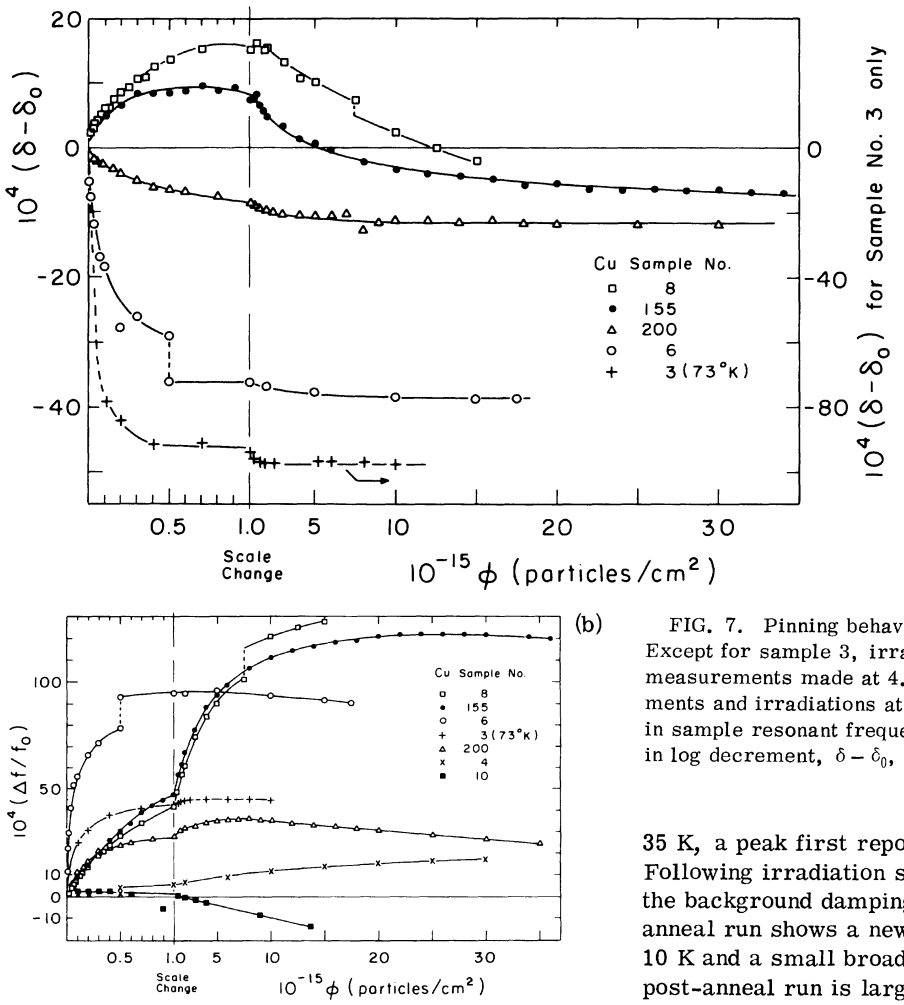


FIG. 7. Pinning behavior of various Cu samples. Except for sample 3, irradiations were at $T \leq 15$ K and measurements made at 4.2 K. Sample 3 had measurements and irradiations at 73 K. (a) Fractional change in sample resonant frequency, $\Delta f/f_0$, vs $\phi$ (b) change in log decrement, $\delta - \delta_0$, vs $\phi$.

applies to the dielastic effect and also to the modulus defect and internal friction associated with stress-induced ordering providing no saturation occurs. The present evidence is that up to fluences of $3\times10^{16}$ protons/cm$^2$ no saturation occurs. The apparent saturation in the 10 K anelastic process in Cu, which was reported earlier,[13] has only been observed for samples whose irradiation has been repeatedly interrupted to monitor changes. The monitoring process is a temperature run up to 16 or 18 K; the small amount of annealing in each run apparently accumulates to give the appearance of a saturation. The energy-loss correction has not been applied to the tables and graphs given below unless it is explicitly noted.

## III. EXPERIMENTAL RESULTS FOR Cu

Figure 2 shows internal friction data typical of moderately cold-worked Cu, in this case a polycrystalline sample. Before irradiation the major structure consists of the Bordoni peak centered near 80 K and a subsidiary peak centered near 30–35 K, a peak first reported by Niblett and Wilks.[12] Following irradiation sufficient to almost remove the background damping observed at 4.2 K, the anneal run shows a new and well defined peak near 10 K and a small broad peak near 30–35 K. The post-anneal run is largely devoid of structure aside from a slight return of the Bordoni peak.

### A. Stress induced ordering in Cu

As reported earlier,[13] an anelastic process has been observed in proton irradiated Cu near a temperature of 10 K. Figure 3 shows the plot of $\delta$ and of $f$ versus temperature for a carefully handled single-crystal Cu sample. Both the fundamental and first overtone results are shown. It was these data that were taken on the second sample probe, so the temperatures are believed accurate to $\pm 0.1$ K. As noted, this sample had the smallest amount of cold work. As shown in Table III, increasing amounts of cold work produced smaller decrement peak heights and modulus defects per unit fluence. For Cu sample 5, which was compressed 25%, no evidence of the low-temperature peak was found.

Annealing of the 10 K peak has been most carefully done on a polycrystalline sample No. 1; no helium gas was used during the 10-min pulse anneals at each temperature. Figure 4 shows the ratio of the peak height after each pulse anneal to the original peak height. Also shown in Fig. 4 are

results of carrying out the anneal on sample Nos. 203, 6, and 7 in 200 mTorr of helium gas. As discussed above, this requires a temperature correction of about −3 K. All such corrected data points are circled on the graph. It seems clear that a pulse anneal to 41 K removes the 10-K peak. The modulus defect annealed out in a very analogous way, but the precision of measurement is much lower.

This 10-K peak was entirely absent in two single-crystal samples oriented with their axes parallel to the ⟨100⟩ crystallographic direction. Figure 5 shows the result of a temperature run for sample 200 which had a ⟨100⟩ orientation and a large fluence just prior to temperature run *a*.

Repeated attempts to observe a stress-induced ordering peak above 20 K, where stage I annealing takes place, were unsuccessful. Our measuring procedures would have required a defect to make about $10^5$ or $10^6$ reorientations in order that they could be detected, so a sufficiently transient defect would not have been observed. Figure 6 shows two attempts in which sample No. 2 was warmed up rapidly (about 1 K/min) following each of two irradiations. The apparent peak in δ centered near 30–35 K is probably a residue of the Niblett-Wilks peak shown in Fig. 2. This peak has a pre-irradiation height of about $50\times10^{-4}$, so only a small fraction needs to remain to account for the broad peak observed in Fig. 6. The sharp frequency increase centered about 40 K is worth noting. The second irradiation and subsequent warm-up resulted in a normal 10-K peak while the 30–35-K peak is greatly diminished in height and the dramatic frequency increase near 40 K is now absent. The large 35-K peak and the 40-K frequency rise are both missing in run *a* for sample 200 (Fig. 5). This sample had a large fluence which seemed to pin all dislocations at the irradiation temperature prior to run *a*.

### B. Fluence dependence of $f$ and δ for Cu

Figure 7 shows the variation of $f$ and δ with fluence for a variety of Cu samples. The $f(\phi)$ graphs [Fig. 7(a)] show an increase usually ascribed to pinning of dislocations followed by a linear decrease which is the dielastic effect. If the linear dependence is extrapolated back to $\phi=0$, the intercept gives the total fractional frequency change produced by pinning. When the linear decrease is not reached during a run, an average dielastic effect is used[11] and the maximum pinning is then estimated. As reported earlier,[11] we have found the dielastic effect to be quite variable from sample to sample but there appears to be no consistent correlation with the amount of CW or with

TABLE V. Pinning rates and amounts.

| Sample | | $10^4\frac{\Delta f_M}{f_0}$ [a] | $10^4\,(\delta_0-\delta)_{max}$ [b] | $10^{15}\frac{d}{d\phi}\left(\frac{f}{\Delta f_M}\right)_0$ [c] | Remarks[d] |
|---|---|---|---|---|---|
| W | 13 | 0.5 | 0.2 | ... | no CW after anneal |
| | 14 | 18 | 2.9 | 12 | no anneal, no CW |
| | 15(F) | 23 | 5.2 | 4.3 | 3% plastic compression |
| | 15(OT) | 20 | 2.2 | 4.0 | |
| | 16(OT) | 10 | 0.9 | 2.7 | 4% plastic comp. |
| | 17 | 17 | 2.1 | 1.3 | 4% plastic comp. |
| | 18 | 5.4 | 0.5 | 1.1 | 5% plastic comp. |
| | 19(F) | 5.4 | 1.1 | 3.2 | 5% plastic comp. |
| | 19(OT) | 3.7 | 1.3 | 1.6 | |
| | 20(F) | 3.0 | 0.6 | 1.1 | 13% plastic comp. |
| | 20(OT) | 2.2 | 0.4 | 2.8 | |
| | 700 | 13 | 2.1 | 1.7 | |
| | 302 | 8.9 | 1.5 | 1.8 | |
| Cu | 10 | 1.3 | 0.2 | 50 ± 40 | CW category 1 |
| | 6 | 96 | 39 | 38 | CW-1 |
| | 8 | 170 | −16 | 0.73 | CW-2, initial rise in δ |
| | 5 | 85 | 8 | 0.23 | CW-3 |
| | 4 | 40 | 0.5 | 0.06 ± 0.03 | 25% plastic comp. |
| | 3 | 45 | 99 | 4.4 | CW-2, liquid-nitrogen data, Bordoni peak is a large factor |
| | 200 | 35 | 40 | 6.6 | CW-2 |

[a] Total fractional frequency change due to pinning.
[b] Total decrement change due to pinning.
[c] Normalized pinning rate at $\phi=0$; value corrected for energy loss.
[d] At 4.2 K unless noted otherwise.

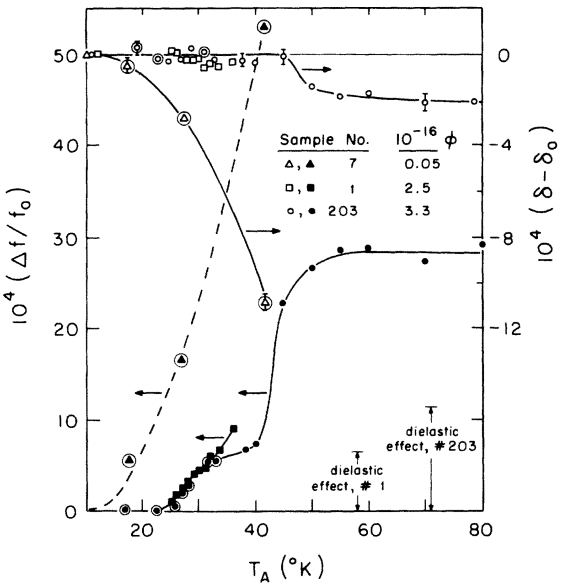


FIG. 8. $\Delta f/f_0$ and $\delta$ as measured at 4.2 K vs anneal temperature for Cu samples irradiated at $T<15$ K. For sample 7, irradiation $T$ was less than 10 K. The arrows show the dielastic effect accumulated by samples 1 and 203.

the crystal orientation.

We have consistently found that the dielastic effect measured during liquid nitrogen runs are at most 10% of the liquid helium results. The effect of CW on the pinning features are dramatic. As shown in Table V, the maximum fractional frequency change varies by a factor of 100 for various samples. Also, the normalized initial pinning rates vary by a factor of 500 or more.

The variation of $\delta$ with $\phi$ is shown in Fig. 7(b) for the same samples. The initial rise in $\delta$ reported by Sosin[4] *et al.* is evident for two of the samples, while the more usual decrease is present for the others. Again, the effect due to CW is large as shown numerically in Table V. Sample 3 was irradiated at 73 K, so pinning of the Bordoni peak was largely responsible for the relatively big change in $\delta$ observed for this sample.

### C. Some annealing results for Cu

Figure 8 shows the changes in log decrement and resonant frequency of polycrystalline Cu sample 1 measured at 4.2 K following a 10-min anneal at each of the temperatures shown. Similar data were taken for sample 203, but as noted above, anneal temperatures below 33 K were measured in about 200 mTorr of He gas. Data points for this sample which have been shifted by minus 3 K are shown circled in Fig. 8.

Also shown in Fig. 8 are the results of annealing a moderately cold-worked sample, No. 7, following a small fluence irradiation at $T<10$ K. This sample was just beginning to show some pinning during its irradiation. The large changes in $f$ and $\delta$ produced by the subsequent annealing result from additional pinning by the thermally activated point defects. It is interesting that sample 7 shows a clearly measurable pinning in both $f$ and $\delta$ below 25 K. By contrast with the small fluence of sample 7, both 1 and 203 had received enough fluence so they had reached the linear dielastic portion of their $f(\phi)$ curve prior to the anneals shown. While frequency changes begin for these samples after anneals as low as 25 K, the absence of a corresponding change in $\delta$ is strong evidence that dislocation pinning is not taking place below 40 K.

## IV. EXPERIMENTAL RESULTS FOR W

Figure 9 shows the preirradiation, anneal, and post-anneal temperature dependence of $\delta$ for a moderately cold-worked high-purity polycrystalline W sample. Two features are different from the corresponding Cu results: the Bordoni peak type of behavior is displaced to a higher temperature (near 140 K) and the anneal run shows four new low-temperature peaks that are then absent during the post-anneal run.

### A. Stress-induced ordering in W

During warm up after irradiation of polycrystalline or single-crystal W, peaks in $\delta$ were observed near 10, 30, 42, and 53 K. The 10- and 53-K peaks were stable at the respective temperatures of the peaks; the 30-K peak lasted about $\frac{1}{2}$ h as it was being observed. Figure 10 shows three different samples during warm-ups following irradiation. The three single-crystal samples were all cut from the same crystal rod, they were similarly treated and mounted, the fluence of 10.1-MeV protons was the same for each, and the rate of warm-up was nearly the same for each. Thus the effect

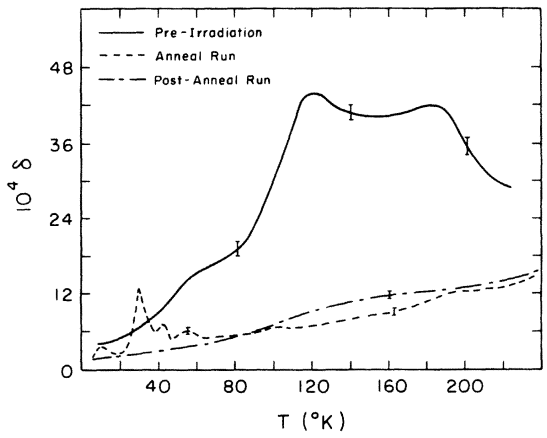


FIG. 9. $\delta$ vs temperature for typical polycrystalline W sample. See Fig. 2 for run definitions.

of changing the stress axis can be observed by comparing the peak heights for these three samples. Table III gives the numerical results.

Following warm-ups above 30 K a small peak began to appear near 14 K. This peak is stable during observation. Figure 11 shows this peak as observed for the fundamental and first overtone frequencies of polycrystalline W sample 302. This peak was also observed in a single-crystal sample. In general it was not observed because of the unusual temperature cycle needed, but it was seen whenever that cycle was carried out. Among the peaks observed in W, this 14-K peak was especially noteworthy because its temperature width (see Table III) agreed closely with that given by Eq. (4).

The 10-K peak in W was also affected by CW. The peak height per unit fluence was greatest for the carefully annealed sample 12 while it was undetectable in sample 15.

In every case where $\delta$ went through a peak, the resonant frequency dropped in the usual manner as illustrated in Fig. 3 for the case of Cu. When observed, overtone peaks were always shifted to higher temperatures (see Table III for data).

### B. Fluence dependence of $f$ and $\delta$ for W

Figure 12 shows the $\phi$ dependence of $f$ and $\delta$ for a variety of W samples. As in the case of Cu, the size of the dielastic effect varied from sample to sample. There was no consistent correlation with CW or with crystal orientation. Because CW was much easier to control in our W samples, the CW dependence of the pinning rate and amounts were studied in some detail. Table V shows first an increase in $\Delta f_{max}/f_0$ as CW increases followed by a sharp decrease in this quantity for large amounts of CW. The initial pinning rate seems to decrease steadily as CW increases. Overall the changes in the pinning behavior with CW were much smaller than in the case of Cu.

### C. Some annealing results for W

The variation of log decrement peak heights with annealing was easily carried out for the stable 10- and 14-K peaks. The 30-K peak was clearly annealing before and after reaching the temperature of observation, so its observed peak heights represent lower limits. Figure 10 shows the 30-K peak on two successive runs (sample 500) at the normal warm-up rate of 1°K/minute; a 30% drop in peak height was observed. This annealing also has the effect of shifting the maximum temperature upwards slightly during successive runs. Figure 13 shows the 10- and 14-K peaks during temperature runs to successively higher maximum anneal

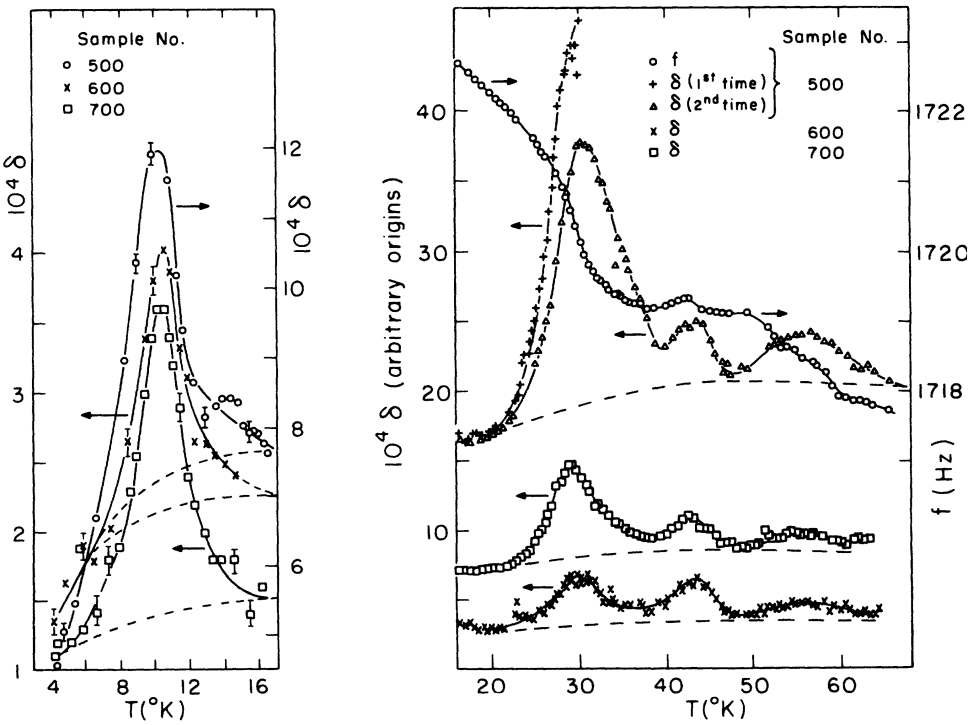


FIG. 10. $\delta$ vs $T$ for three single-crystal W samples. Preparation and irradiations were as identical as possible for three samples. $f$ vs $T$ is shown for the first run of sample 500; very similar $f(T)$ results were found for the other samples. Assumed backgrounds are shown as dashed lines.

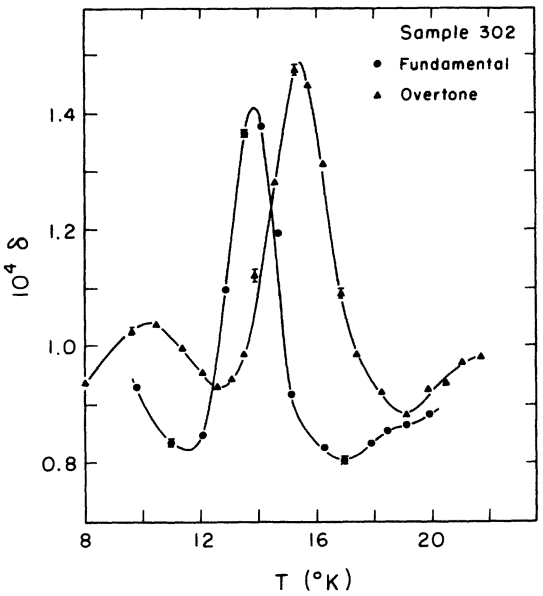


FIG. 11. $\delta$ vs $T$ for W sample 302 showing 14-K peak after the sample had been annealed to 47 K.

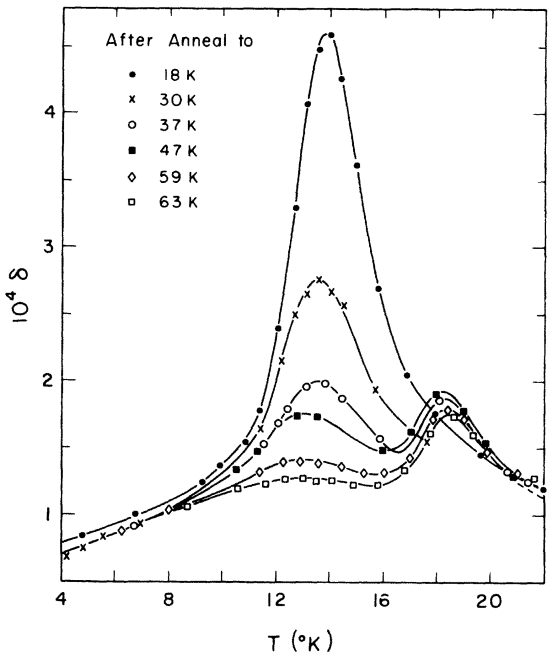


FIG. 13. Successive temperature runs for $\delta$ of sample 302 overtone.

temperatures. These data show the peaks occurring at relatively high temperatures because they were observed in the presence of 200 mTorr of helium and the sample frequency of 4840 Hz was fairly high. It is evident that the background subtraction

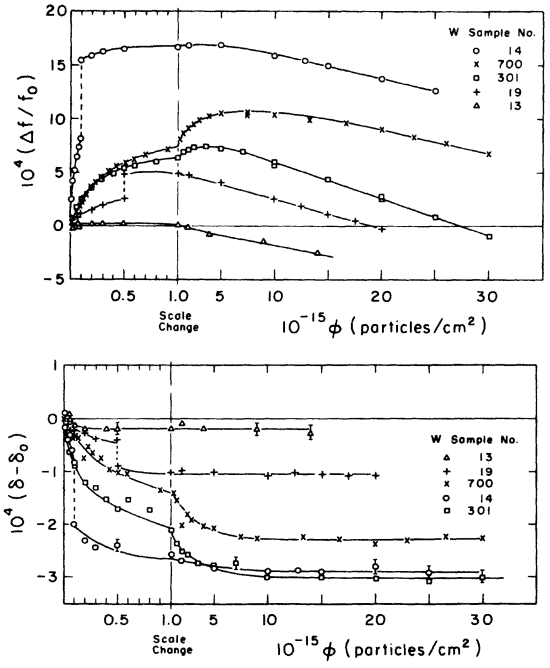


FIG. 12. For some W samples, the fluence dependence of $f$ [Fig. 12(a)] and of $\delta$ [Fig. 12(b)]. All irradiations at $T \leq 15$ K, measurements at 4.2 K.

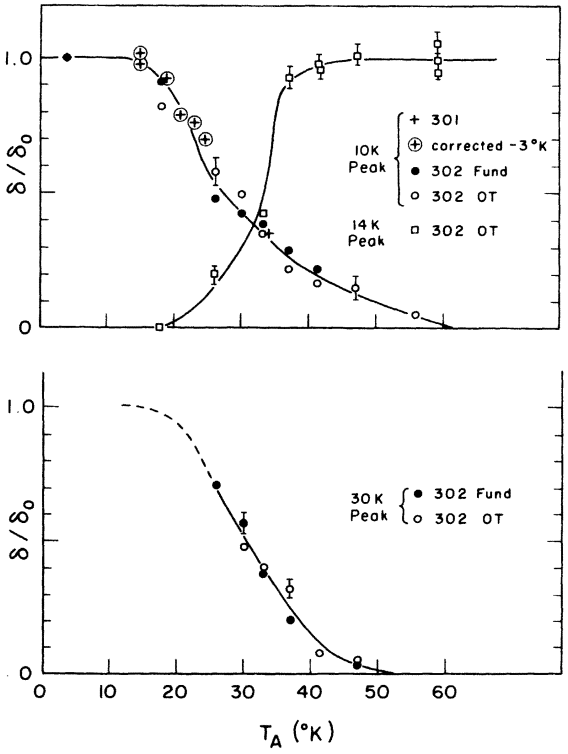


FIG. 14. Normalized heights of $\delta$-vs-$T$ peaks in W samples following irradiation and anneals to temperatures shown; $\delta_0$ is the peak height observed the first time after irradiation. For the 30-K peak, $\delta_0$ has been multiplied by 1.3. (F denotes fundamental, OT denotes first overtone.)

for the 10-K peak becomes difficult after the anneal run to 37 K. The normalized peak heights for the 10- and 14-K peaks are shown in Fig. 14 as a function of the maximum anneal temperature. Also shown are the results for the 30-K peak height; here the normalization height $\delta_0$ is chosen as the height achieved during the first scan times a factor of 1.3 to correct approximately for the height loss during the first scan. It is evident that the 14-K peak is growing in just the temperature range where the 30-K peak is annealing; the 10-K peak is also disappearing in this range but has a substantial high-temperature component which persists to an annealing temperature of 55 K. This component may be an artifact due to the background problem shown in Fig. 13.

The changes in decrement and frequency, as measured at 4.2 K after irradiation and a subsequent anneal to various temperatures, are shown in Fig. 15. Samples 11, 301, 302 were all given large fluences; their dislocations were effectively pinned prior to the data shown. This is especially true for 302 which was radiation doped with $1\times10^{16}$ protons/cm$^2$ and then annealed at 50 K. By contrast, sample 15 received only $3\times10^{13}$ protons/cm$^2$ prior to its anneal. Despite this low fluence, annealing produced frequency and decrement changes nearly ten times as large as those seen in the heavily irradiated samples. For both types of sample the frequency changes become measurable at a temperature very close to 18 K.

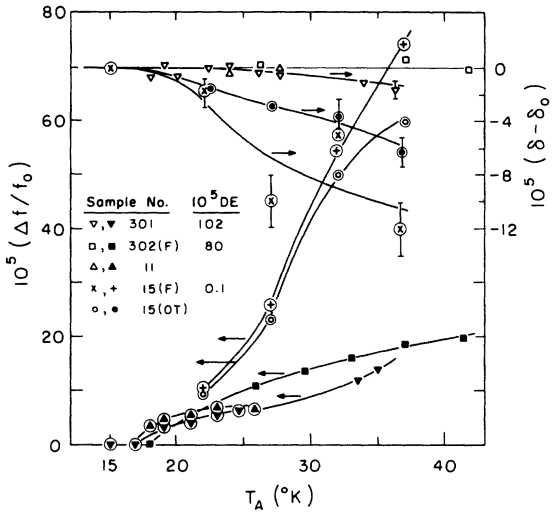


FIG. 15. $\Delta f/f_0$ and $\delta$ as measured at 4.2 K versus anneal temperature for W samples irradiated at $T<15$ K. The accumulated dielastic effect (DE) is shown for samples in units of $\Delta f/f_0\times10^5$; it was not obtained for No. 11.

## V. DISCUSSION OF RESULTS

### A. Defect concentrations

The lattice defects produced by 10-MeV protons or deuterons in W and Cu are the result of Rutherford scattering because the Coulomb barriers are sufficient to prevent any significant number of nuclear reactions. By postulating a minimum energy transfer to a lattice atom in order to produce a displacement, the number of primary knock-on atoms can be calculated.[14] If $E_T$ is the threshold energy transfer, then a fluence of $10^{16}$ 10 MeV protons/cm$^2$ will result in the following:

$$\text{for Cu,}\quad \gamma_0=(8.61\times10^{-4})/E_T=3.45\times10^{-5}\ ,$$
$$\text{for W,}\quad \gamma_0=(1.94\times10^{-3})/E_T=4.2\times10^{-5}\ , \tag{7}$$

where $E_T$ has been taken as 25 eV for Cu[15] and 47 eV for W[16] and $\gamma_0$ is the fraction of lattice atoms per $10^{16}$ fluence receiving a recoil energy in excess of $E_T$ directly from the incident protons. Half of these collisions produce no secondary displacements because the energy transferred is between $E_T$ and $2E_T$. Various theoretical estimates of the number of secondary displacements averaged over all collisions predict that the values in Eq. (7) should be multiplied by a factor close to 5.[14]

This simple calculation is of value for crude estimates, but it leaves out a number of complications ranging from a directional dependence of $E_T$ to the effect of focussing collisions and interstitial-vacancy ($I-V$) recombinations. The over-all effect of these complications has been measured for 10-MeV protons in Cu by Nilan and Granato.[15] They concluded that Eq. (7), without any factor for secondary displacements, gives the atomic fraction of $I-V$ pairs that anneal out in stage I produced by $10^{16}$ protons/cm$^2$. More detailed information on the close pair concentrations after deuteron irradiation to $2\times10^{16}$ deuterons/cm$^2$ was given by Magnuson *et al.*[17] From their distribution of activation energies, one can conclude that 11% of the stage I defect resistivity is associated with stage $I_B$ having an activation energy near 0.091 eV. Assuming their state of damage is close to that which we observe, we conclude that $\gamma_B=3.9\times10^{-6}$ per $10^{16}$ protons/cm$^2$; the precision of this result is estimated to be ±20%.

No corresponding proton studies have been made for W. The electron results of DiCarlo *et al.* can, however, be used to get some estimate. For three different ⟨100⟩ oriented W crystals they measured $\delta_{30\ K}$, the height of the 30-K internal friction peak per unit fluence of electrons. Their result was $(5.0\pm1)\times10^{-22}$ cm$^2$/electron. They also observed the electrical resistivity which annealed out near the 30-K peak; they concluded it corresponded to an atomic fraction of defect pairs $\gamma_{30\ K}=(1.5\pm0.5)\times10^{-23}$ cm$^2$/electron. Thus we find $\gamma_{30\ K}=(33\pm8)\delta_{30\ K}$; this enables us to use the data for the

⟨100⟩ crystal in Fig. 10 to estimate $\gamma_{30\ K}$ for 10 MeV protons. This comparison of transient peak heights is justified because the rate of temperature rise was close to 1 K/min both for the electron and for the present proton data. For $10^{16}$ protons/cm$^2$ this intercomparison gives $\gamma_{30\ K}=(1.9\pm0.4)\times10^{-5}$, a figure used below in interpreting the 30-K peak. Finally, DiCarlo *et al.* estimated that $\gamma_{30\ K}$ was about $\frac{1}{6}$ of the total pair concentration. This would predict $\gamma\simeq1\times10^{-4}$ per $10^{15}$ protons/cm$^2$, about a factor of 2 larger than Eq. (7) predicts. This is certainly adequate agreement in view of the differences expected between the defect distributions produced by electron and proton irradiation.

### B. Stress-induced ordering

The most direct quantities that can be determined from the Debye relaxation effects are $\nu_0$ and $Q_r$ as defined in Eq. (1). As seen from Eq. (2), $\delta$ has its maximum value of $\frac{1}{2}\pi\Delta_0$ when $\omega\tau=1$. By expressing $\omega\tau=1$ in terms of the measured angular frequencies $\omega_1$ and $\omega_2$ for two different resonant modes of the sample and the two temperatures $T_1$ and $T_2$ where these modes show a maximum $\delta$, one finds

$$Q_r=\frac{kT_1T_2}{T_2-T_1}\ln\left(\frac{\omega_2}{\omega_1}\right),$$
$$\log_{10}\nu_0=\log_{10}\omega_2+\frac{T_1}{T_2-T_1}\log_{10}\left(\frac{\omega_2}{\omega_1}\right). \tag{8}$$

When these equations are applied to the fundamental and overtone modes of a sample during the same warm-up run, the systematic temperature errors are essentially the same for both $T_1$ and $T_2$. The systematic error in $T_2-T_1$ is then greatly reduced thereby reducing the systematic error in $Q_r$ and $\nu_0$. Table IV shows values of $Q$ and $\log_{10}\nu_0$ for all runs on W wherein the helium exchange gas pressure was 10 mTorr or less; the systematic temperature errors are therefore less than 0.5 K. The Cu data, also noted in the table, were either taken on the new probe or were corrected for temperature errors; again the corrected values are within 0.5 K.

The frequency factors for reorientation $\nu_0$ are related to atomic jump attempt frequencies $\nu_j$ by the number of ways in which atomic jumps can result in reorientation.[1] For the Cu 10-K defect, Holder *et al.*[8] have proposed a model in which only two positions are available so $\nu_j=\frac{1}{2}\nu_0$. For a ⟨110⟩ orientation, which has been assumed here for the W defects, Nowick and Berry's method[1] (their Eqs. 8.9-19) gives $\nu_j=\frac{1}{6}\nu_0$. Applying these factors to the $\nu_0$ values in Table IV for the 10-K peaks, we find $\nu_j=3\times10^{(11\pm1)}$ for Cu and $\nu_j=1\times10^{(11\pm0.5)}$ for the W peak. These attempt frequencies are small compared with the corresponding Debye frequencies of about $7.5\times10^{12}$ Hz for both Cu and W. Wiener[18] has proposed a quantum theory of rate processes which predicts an attempt frequency $f'=1.98kT/h$ for temperatures well below the Debye temperature. For $T=10$ K, $f'=4.1\times10^{11}$ Hz, which is close to the values of $\nu_j$ obtained here. Since $\nu_0$ also includes an unknown entropy of activation factor, the approximate agreement noted here can only be suggestive at this time.

#### *1. Cu 10-K peak*

The annealing of the Cu 10-K peak, as shown in Fig. 4, begins above 22 K and is essentially complete by the time 41 K is reached. This clearly associates the defect with stages $I_B$ or $I_C$ as reported earlier.[13] The new data on samples 1, 6, and 8 plus the corrected temperatures for No. 203 place the temperature of maximum recovery rate between 27 and 29 K. This is close to stage $I_B$ which, for electrical resistivity, has a maximum recovery rate at 27 K for 10-min isochronal annealing.

The Cu 10-K peak was surprisingly sensitive to cold work. As the amount of cold work increased, the peak height per unit fluence dropped continuously (see Table III). A sample which had been compressed by 25% failed to show any evidence of this peak in $\delta$ or of any corresponding frequency drop. The gradual disappearance with cold work seems explicable in terms of interactions with dislocations. The strain fields of edge dislocations, well away from the core, can be approximated by $\epsilon_d=b/2\pi r$, where $b$ is the Burger's vector and $r$ the radial distance from the core. The interaction energy between a defect and the dislocation is given by $\epsilon_d P$ where $P$ is the elastic double force strength estimated for Cu to be about 2 eV by Seeger *et al.*[19] When this interaction energy exceeds $kT$, then the defect's orientation is essentially unaffected by thermal activation and a small external stress will no longer produce internal friction. For $T=10$ K and $P=2$ eV, we find $r\simeq400b$ as the radius within which defects are immobilized. When the average spacing of dislocations is $800b$, then essentially all defects are immobilized against reorientation. For Cu this would require about $10^9$ to $10^{10}$ dislocations/cm$^2$, a reasonable value for a heavily cold-worked metal.

Because the 10-K defect is absent from samples with ⟨100⟩ orientation, we assume it has trigonal symmetry. Use is made of Eq. (5) in conjunction with $\psi_{111}^{111}$ from Table I, $C$ from $\gamma_B=3.9\times10^{-6}$ atomic fraction per $10^{16}$ fluence, Young's Modulus $E$ is used for $M^{[hkl]}$,

$$E^{111}=3\left(\frac{1}{C_{11}+2C_{12}}+\frac{1}{C_{44}}\right)^{-1}=2.06\times10^{12}\ \text{ergs/cm}^3,$$

and $\Delta_0=5.5\times10^{-4}$ per $10^{16}$ fluence is taken from

sample 37. This choice of $\Delta_0$ from the least cold-worked sample follows from the systematic decrease in $\Delta_0$ discussed above. The value used is based upon the frequency change because it is less sensitive to strain broadening than is the internal friction peak height. The result is $|\lambda_1 - \lambda_2| = 0.20 \pm 0.02$, the uncertainty largely a result of the calculation of $\gamma_B$. Holder *et al.* have also estimated $\Delta\lambda$; assuming a $I_B$ defect, their value becomes $\Delta\lambda = 0.17$.[20] The small discrepancy may well result from their $\Delta f$ measurement which is made up to 25 K where annealing has begun thus reducing the observed frequency change. Wenzl[6] has used a variety of Cu stage I annealing studies to conclude that the strain induced volume change associated with a stage I defect is +1.9 atomic volumes. In terms of the $\lambda$ tensor this means $\lambda_1 + \lambda_2 + \lambda_3 = 1.9$. For the present case, taking $\lambda_1 > \lambda_2$ and $\lambda_2 = \lambda_3$, we can determine that $\lambda_1 = 0.77$ and $\lambda_2 = 0.57$ with estimated uncertainties of about 5%.

### 2. W peaks

The results for the W peaks can be compared in part with those of DiCarlo *et al.* We confirm their conclusion that the 30-K peak is associated with a defect having a ⟨110⟩ axis of symmetry; this seems also to be true for the 10-K and possibly for the 53-K peaks. Using the peak heights of samples 500, 600, and 700 from Table III and the procedures described by DiCarlo *et al.* (their Secs. B-2 and 3) for refining the observed peak height ratios, we obtained the results shown in Table IV for these ratios. For the 10- and 30-K peaks the refinement process gives ratios quite consistent with the observed ratios. When applied to the 53-K results, however, the "refined ratios" are quite inconsistent with the observed ratios. It seems probable, therefore, that the 53-K peak does not arise from a simple defect with orthorhombic symmetry, but rather from a more complex defect. This is also made plausible by the fact that substantial atomic motion has taken place below 53 K as evidenced by the peak annealing data of Fig. 14.

To convert the $\Delta_0$ ratios into shape factors for the 10-K peak, use is made of the $\Delta_0^{110}$ value found from $\Delta f/f$ of sample 12, the sample which was our least cold-worked W sample. For the 30-K peak, use is made of $\Delta_0^{100}$ from the internal friction peak height of sample 500 multiplied by 1.3 to approximately correct for annealing as discussed above. For both peaks use is then made of Eq. (5) with $M = 4.1 \times 10^{12}$ ergs/cm$^3$ and $C = \gamma_{30\ \mathrm{K}}$ equal to $(1.9 \pm 0.4) \times 10^{-5}$. The resulting shape factors are given in Table IV. To complete the determination of the $\lambda$ tensor, use is made of the strain induced volume change for a split interstitial in W as calculated by Stabell[21]: $v = 0.87 v_0$. Setting $\lambda_1 + \lambda_2 + \lambda_3 = 0.87$, together with the shape factors of Table IV, gives the $\lambda$ components. Although the shape factors (which are known to ±10%) are distinctly different, they are small and the two $\lambda$ tensors are very similar.

In finding these $\lambda$ values, $\gamma_{30\ \mathrm{K}}$ was used for the atomic fraction of the 10 K defects as well. This seems justified in view of the similar annealing behavior shown in Fig. 14. It assumes that the 10-K peak arises from the reorientation of a defect which does not become mobile until 30 K where it both reorients and migrates. Since no estimate of $\gamma_{53\ \mathrm{K}}$ is available, no $\lambda$ values could be calculated.

For sample 351, after a total proton fluence of $9.5 \times 10^{16}$, the 30-K peak was observed isothermally at the peak temperature. The peak half-life was estimated at 15 min. Since the sample frequency was 746 Hz, the reorientation jump rate was $2(746) = 4.68 \times 10^3$ Hz; the defect therefore made about $4.2 \times 10^6$ reorientations before being removed by a sink. At this level of fluence, the vacancy concentration was about $4 \times 10^{-4}$ so each reorientation cannot correspond with a lattice jump or the defect would typically annihilate itself after about 2500 reorientations. A plausible interpretation is that reorientation jumps vastly outnumber lattice migration jumps. Barring extraordinary entropy factors, it can then be concluded that

$$\frac{\text{reorientation jumps}}{\text{migration jumps}} = \frac{\exp(-Q_r/kT)}{\exp(-Q_a/kT)} = \frac{4.2 \times 10^6}{2500},$$

where $Q_a$ is the activation energy for a lattice jump. Solving this equation for $Q_a$ gives $Q_a = 0.077$ eV based upon the value of $Q_r$ from Table IV. This estimated value of $Q_a$ is in good agreement with the estimate by Seidman[22] who obtained $0.08 \pm 0.01$ eV. Our estimate for $Q_a$ represents a lower limit because the number of lattice jumps to annihilate will be decreased below 2500 by correlation between the initial positions of the interstitials and vacancies and by the presence of other sinks. This viewpoint would also explain the observation by DiCarlo *et al.* that the 30-K peak height was insensitive to radiation doping; making many reorientations before migrating will assure that the peak is detected before the defect has annealed away.

## C. Low-temperature anneal

As the sample temperature is increased following irradiation, the type and amount of annealing depends strongly on whether the dislocations have been essentially pinned by the irradiation. In Fig. 8, Cu samples 1 and 203 have received enough irradiation to have induced a sizeable dielastic effect. Annealing to 40 K produces a recovery in the frequency measured at 4.2 K which is close in magnitude to the dielastic effect. By contrast, sample 7, which has just begun to be pinned by its irradiation, experiences a large anneal in $f$ and $\delta$

induced by the thermally activated defects migrating to the unpinned dislocations. As with a number of samples treated similarly, sample 7 displays pinning-type behavior for anneals well below 30 K. These effects cannot arise from long-range migration, so they presumably result from localized reorientations of defects which then become more effective as dislocation pinners.

The results shown in Fig. 6 offer the most direct evidence that the Cu dielastic effect anneals out in stage I. As detailed in the figure caption, an irradiation followed by an anneal to 80 K raised the frequency at 4.2 K to $f_1$ on the graph. A second irradiation resulted in a dielastic effect which lowered the frequency to $f_2$. Two successive temperature runs up to 60 K then resulted in the frequency returning to $f_1$. This behavior is in agreement with observations by Rehn *et al.*[7]

The anneal behavior of sample 203 in Fig. 8 shows a decrease in $\delta$ and a frequency increase greater than the dielastic effect. That these changes would occur is evidence of further pinning even though the sample clearly showed the linear decrease at large $\phi$ values. Having observed this effect in other Cu samples, we conclude that irradiation near 10 K does not totally pin some dislocations. The apparent persistence of the Niblett Wilks peak in $\delta$ near 35 K is further evidence of this difficulty in complete pinning by low-temperature irradiations.

Figure 15 shows the recoveries in $f$ and $\delta$ at 4.2 K for W during low-temperature anneals. The absence of changes in $\delta$ for the high fluence samples 11, 301, and 302 is strong evidence that dislocation pinning is not taking place. The amount of frequency recovery in these samples is only about $\frac{1}{3}$ of their dielastic effects, so the evidence suggests an annealing of the dielastic effect beginning near 18 K and continuing on past 40 K. As seen in Fig. 14, this is just the temperature range in which the 10- and 30-K peaks in $\delta$ are disappearing.

As in the case of Cu, a low fluence W sample such as 15 shows clear evidence of dislocation pinning in this low-temperature anneal region. In the corresponding data for Cu (Fig. 8) it was evident that dislocation pinning was taking place before long-range migration in stages $I_D$ and $I_E$ was occurring. As a consequence it is difficult to interpret the W results in Fig. 15 to decide upon a temperature for long-range interstitial migration.

### D. Dislocation pinning

The most striking feature of the dislocation pinning data is the large effect produced by cold work. Table V shows the amount of total pinning observed for various samples as measured by the fractional change in resonant frequency and by the change in the log decrement. In W the amount of pinning at 4.2 K reaches a peak value at a compression of about 4% followed by a large decrease in pinning at larger compressions. By contrast, the amount of pinning in Cu at 4.2 K initially increases with the amount of cold work and then remains fairly constant. In addition to changing the amount of pinning, cold work also affects the rate of pinning. The initial pinning rates are also shown in Table V, and they are seen to vary by a factor of 500 for Cu and 10 for W depending upon the state of cold work.

Both of these effects on pinning are qualitatively explicable using the random pinning model.[3] The amount of pinning increases with cold work due to the introduction of more dislocations until dislocations begin to restrict the motion of one another. In the case of Cu these two effects roughly compensate one another for large amounts of cold work. In the case of W, the restriction of motion seems to be dominant above 3% or 4% compression. The pinning rate is much larger for long dislocations, according to the random pinning model. As cold work continues to build up, dislocation loops get shorter due to point defects and to the production of dislocation networks.

The random pinning model is also successful in qualitatively explaining the large effect on the pinning rate due to the temperature of irradiation. If point defects are mobile at the temperature of irradiation, then they can migrate to dislocations and pin them. With their carefully annealed specimens, Thompson and Pare[3] report pinning rates which increase by a factor of 100 between 20 and 78 K. By contrast with this result, our moderate to heavy cold-worked samples show pinning rates which differ by less than a factor of 2 between 15 and 73 K. It would seem that thermally activated defect mobility is much less important for dislocation pinning in samples with substantial amounts of cold work. Aside from the rare events in which a defect is produced very near the core of a dislocation, lattice events such as dynamic crowdions, focussons, or defect cascades[23] can produce pinning which is insensitive to the temperature of irradiation. As the dimensions of the dislocation loops become smaller, as CW increases, the results reported here suggest that dynamic lattice events will become progressively more important in the pinning process.

## VI. CONCLUSIONS

For Cu, the anelastic process observed near 10 K after irradiation is identified with the defect which anneals in stage $I_B$. The shape factor $|\lambda_1 - \lambda_2|$ was measured to be $0.20 \pm 0.02$, a result which agrees well with a revised value due to Holder *et al.* Values of $\lambda$, $Q_r$, and $\nu_0$ are all given

in Table IV. When samples with a large fluence are annealed up to 45 K, they show a recovery of their elastic modulus measured at 4.2 K which is comparable with the accumulated dielastic effect. This result indicates the stage I defects are responsible for the dielastic effect in agreement with the suggestions of Holder *et al.* Annealing in stages $I_D$ and $I_E$ showed dramatic dislocation pinning in low and moderate fluence samples, but no clear evidence of stress-induced ordering was found in this temperature region. This may be a consequence of the present experiment being insensitive to defects making fewer than $10^5$ to $10^6$ reorientations before disappearing.

For W, five stress-induced ordering processes were observed after proton irradiation near 10 K. One of these, causing a peak near 14 K, only arises after annealing to a temperature where other peaks near 10 and 30 K have begun annealing. This behavior is similar to that observed by Okuda and Mizubayashi[24] for a peak near 8 K in neutron irradiated Mo after it had been annealed above 45 K. The same authors[25] have recently reported some measurements at 500 Hz on neutron irradiated W in which they observe peaks at 8 and 27 K. Their estimated defect concentration of $6\times10^{-5}$ at fraction is close to that of the samples reported here; their peak heights coincide very well with those given in our Table III for the 10- and 30-K peaks. It therefore seems most unlikely that their 8-K peak is different from our 10-K peak as they suggest. Also, their suggestion that these two peaks represent two distinct annealing stages is inconsistent with our Fig. 14 which shows the 10- and 30-K peaks annealing away over the same temperature range. Within ±2 K, their peak positions and the beginning of the anneal process agree well with the results reported here. These authors[25] conclude from their observed frequency increase that long-range interstitial migration takes place during annealing near 15 K. From our results with Cu (Fig. 8) it seems evident that dislocation pinning can occur at temperatures below that at which long-range interstitial migration begins. From the behavior of the peaks in W shown in Fig. 14, we can conclude that annealing near 30 K causes defects to disappear and produces new defects such as the ones responsible for the 14-K peak.

An anneal to 50 K does not remove the dielastic effect in W as it appears to do in Cu; only about $\frac{1}{3}$ of the effect is removed in the case of W. This suggests that other polarizable defects may remain which are stable to higher temperatures. Two candidates for this role are the defects associated with the 14- and 53-K peaks; they begin to anneal only above 70 K.

The processes observed near 10 K in both Cu and W proved to be sensitive to cold work. For both materials the largest relaxation strengths per unit fluence were found in carefully annealed specimens. Increasing CW produced a decrease in the internal friction peaks and in the modulus defect until the effect was eliminated entirely by heavy CW. This seems explicable by the increased interaction between the point defects and the dislocations. A second effect of CW on both materials was the change in the pinning behavior. Pinning amounts and initial pinning rates vary by a factor of 500 in Cu and a factor of 10 in W as the amount of CW changes. The pinning rates in CW samples seem far less temperature dependent than has been reported for well annealed samples.

## ACKNOWLEDGMENTS

The authors gratefully acknowledge the vital cooperation of the Nuclear Physics Laboratory personnel. Access to the Van de Graaf accelerator was made possible by the NSF support of that facility. The use of unpublished data from R. L. Nielsen and D. E. Stabell is also acknowledged.

---

†Research supported by the NSF under Grant No. GH-31991.

*Present address: Navy Eastern Standard Laboratory, Washington, D. C.

‡Present address: Physics Dept., Old Dominion University, Norfolk, Va.

[1]A. S. Nowick and B. S. Berry, *Anelastic Relaxation in Crystalline Solids* (Academic, New York, 1972).

[2]J. A. DiCarlo, C. L. Snead, and A. N. Goland, Phys. Rev. 178, 1059 (1969).

[3]D. O. Thompson and V. K. Pare, in *Physical Acoustics* edited by W. P. Mason (Academic, New York, 1966), Part IIIA, p. 293.

[4]H. M. Simpson, A. Sosin, and S. L. Seiffert, J. Appl. Phys. 42, 3977 (1971).

[5]V. K. Pare and H. D. Guberman, J. Appl. Phys. 44, 32 (1973).

[6]H. Wenzl, in *Vacancies and Interstitials in Metals*, edited by A. Seeger, D. Schumacher, W. Schilling, and J. Diehl (North-Holland, Amsterdam, 1970).

[7]L. E. Rehn, J. Holder, A. V. Granato, R. R. Coltman, and F. W. Young, Jr., Phys. Rev. B 10, 349 (1974).

[8]J. Holder, A. V. Granato, and L. E. Rehn, Phys. Rev. B 10, 363 (1974).

[9]J. A. DiCarlo and J. R. Townsend, Acta Metall. 14, 1715 (1969).

[10]J. C. Swartz, Rev. Sci. Instrum. 35, 1573 (1964).

[11]J. R. Townsend, J. A. DiCarlo, R. L. Nielsen, and D. Stabell, Acta Metall. 17, 425 (1969).

[12]D. H. Niblett and J. Wilks, Philos. Mag. 2, 1427 (1957).

[13]R. Nielsen and J. R. Townsend, Phys. Rev. Lett. 21, 1749 (1968).

[14]F. Seitz and J. S. Koehler, *Advances in Solid State Physics* (Academic, New York, 1956), Vol. 2, p. 305.

[15]T. G. Nilan and A. V. Granato, Phys. Rev. 137,

A1233 (1965).
[16]C. G. Roberts and P. E. Shearin (private communication).
[17]G. D. Magnuson, W. Palmer, and J. S. Koehler, Phys. Rev. 109, 1990 (1958).
[18]J. H. Wiener, Phys. Rev. 169, 570 (1968).
[19]A. Seeger, E. Mann, and R. V. Jan, J. Phys. Chem. Solids 23, 639 (1962).
[20]J. Holder, A. V. Granato, and L. E. Rehn in private communications, confirm this revised value of $\Delta\lambda$.
[21]D. Stabell and J. R. Townsend, Acta Metall. 22, 473 (1974).
[22]D. N. Seidman, J. Phys. F 3, 393 (1973).
[23]M. W. Thompson, *Defects and Radiation Damage in Metals* (Cambridge U.P., Cambridge, England, 1969), Chap. 5.
[24]S. Okuda and H. Mizubayashi, Cryst. Lattice Defects 4, 75 (1973).
[25]S. Okuda and H. Mizubayashi, Phys. Rev. Lett. 34, 815 (1975).